

[(O \wedge N \wedge N)PtX] Complexes as a New Class of Light-Emitting Materials for Electrophosphorescent Devices

Chi-Chung Kwok, Hugo M. Y. Ngai, Siu-Chung Chan, Iona H. T. Sham, Chi-Ming Che,* and Nianyong Zhu

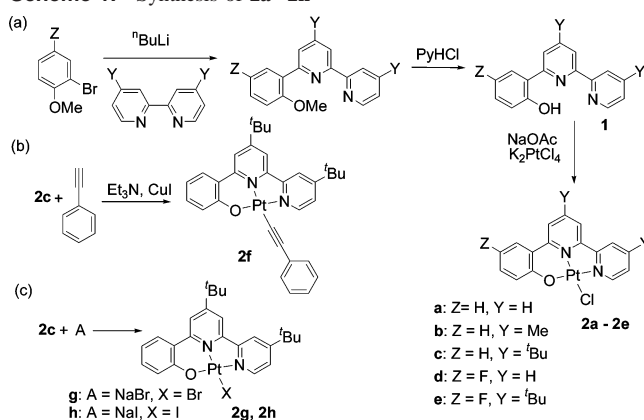
Department of Chemistry and the HKU-CAS Joint Laboratory on New Materials, The University of Hong Kong, Pokfulam, Hong Kong Special Administrative Region, China

Received March 10, 2005

The synthesis and photophysical properties of the robust Pt(II) emitters [(O \wedge N \wedge N)PtX] (HO \wedge N \wedge N = 6-(2-hydroxyphenyl)-2,2'-bipyridine and its derivatives; X = Cl, Br, I, or $-C\equiv C-Ph$) are reported. Yellow electroluminescent devices based on these materials display a low turn-on voltage (1 cd m $^{-2}$ at 4 V) and a high luminance (37000 cd m $^{-2}$). Complex **2e**, [(F t Bu $_2$ O \wedge N \wedge N)-PtCl], has the highest thermal stability and gave the best OLED.

The application of platinum(II) chelates as electrophosphorescent emitters has recently been demonstrated to impact the development of high-performance organic light-emitting devices (OLEDs).^{1–6} Until now, most Pt(II) chelates used for this purpose (i) have a tetradentate ligand, such as [Pt(N $_2$ O $_2$)] (H $_2$ N $_2$ O $_2$ = bis(2'-phenol)bipyridines or -phenanthrolines),² Pt Schiff base,³ and Pt porphyrin complexes;⁴ (ii) are cyclometalated, for example, [(C \wedge N)Pt(O \wedge O)] (C \wedge N = 2-phenylpyridyl, 2-(2'-thienyl)pyridyl or 2-(4,6-difluorophenyl)pyridyl; O \wedge O = β -diketonato)⁵ and [(C \wedge N \wedge N)-PtR]⁺ (HC \wedge N \wedge N = 6-aryl-2,2'-bipyridine);⁶ and, more recently, (iii) contain bidentate N–N donor ligands such as [Pt(iqdz) $_2$] and [Pt(pydz) $_2$] (iqdz = isoquinolinyl indazole, pydz = pyridyl indazole).¹ Previous work demonstrated that [Pt(N $_2$ O $_2$)] complexes are robust emitters with good thermal stability, as ensured by the chelating effect of the H $_2$ N $_2$ O $_2$ ligand.² The shortcoming, however, stems from the synthesis

Scheme 1. Synthesis of **2a–2h**



and purification processes, which involve a number of steps, resulting in overall low product yields.

One of the side products obtained in the synthesis of H $_2$ N $_2$ O $_2$ ligand is HO \wedge N \wedge N (6-(2-hydroxyphenyl)-2,2'-bipyridine). We envision that (O \wedge N \wedge N)-type complexes of Pt(II) could be readily prepared, would exhibit thermal stability, and are potential emitters for optoelectronic devices. The physical properties of these [(O \wedge N \wedge N)PtX] complexes (**2a–2h**, X = Cl, Br, I, or $-C\equiv C-Ph$, Scheme 1) should be easily modified through the non-chelated auxiliary ligand X, as opposed to the difficulty of modifying the N $_2$ O $_2$ chelate in the [Pt(N $_2$ O $_2$)] complexes.

Complexes **2a–2e** were obtained, in 68–85% yields, by reacting a DMF (*N,N'*-dimethylformamide) solution of the corresponding HO \wedge N \wedge N ligand (**1a–1e**) and sodium acetate with a DMSO (dimethyl sulfoxide) solution of K $_2$ PtCl $_4$ at 60 °C.^{7,8} Complexes **2f–2h** were prepared by substituting the Cl ligand in **2c** with phenylacetylide, Br, or I, respectively (Scheme 1). Purification of **2a–2f** was achieved by washing with CH $_2$ Cl $_2$, water, and MeOH, whereas **2g** and **2h** were purified by chromatography on a silica gel column with CH $_2$ Cl $_2$ as the eluent.

(7) Holligan, B. M.; Jeffery, J. C.; Ward, M. D. *J. Chem. Soc., Dalton Trans.* **1992**, 23, 3337–3344.

(8) Jeffery, J. C.; Schatz, E.; Ward, M. D. *J. Chem. Soc., Dalton Trans.* **1992**, 12, 1921–1927.

* To whom correspondence should be addressed. E-mail: cmche@hku.hk.

(1) Kavitha, J.; Chang, S. Y.; Chi, Y.; Yu, J. K.; Hu, Y. H.; Chou, P. T.; Peng, S. M.; Lee, G. H.; Tao, Y. T.; Chien, C. H.; Carty, A. J. *Adv. Funct. Mater.* **2005**, 15, 223–229.

(2) Lin, Y. Y.; Chan, S. C.; Chan, M. C. W.; Hou, Y. J.; Zhu, N.; Che, C. M.; Liu, Y.; Wang, Y. *Chem. Eur. J.* **2003**, 9, 1263–1272.

(3) Che, C. M.; Chan, S. C.; Xiang, H. F.; Chan, M. C. W.; Liu, Y.; Wang, Y. *Chem. Commun.* **2004**, 1484–1485.

(4) Wang, X.; Andersson, M. R.; Thompson, M. E.; Inganäs, O. *Thin Solid Films* **2004**, 468, 226–233.

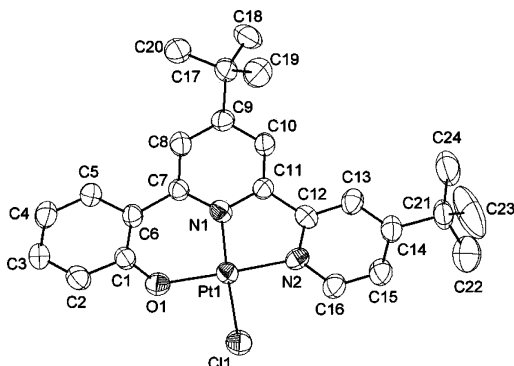
(5) Brooks, J.; Babayan, Y.; Lamansky, S.; Djurovich, P. I.; Tsyba, I.; Bau, R.; Thompson, M. E. *Inorg. Chem.* **2002**, 41, 3055–3066.

(6) Lu, W.; Mi, B. X.; Chan, M. C. W.; Hui, Z.; Zhu, N.; Lee, S. T.; Che, C. M. *Chem. Commun.* **2002**, 206–207.

Table 1. Physical Data for **2a–2h**

	$T_d^a/^\circ\text{C}$	E_{pa}^b/V	$E_{1/2}^{\text{redc}}/\text{V}$	HOMO/eV	LUMO/eV
2a	388	0.81	-1.76	-5.61	-3.04
2b	421	0.86	-1.83	-5.66	-2.97
2c	425	0.82	-1.85	-5.62	-2.95
2d	351	0.68	-1.69	-5.48	-3.11
2e	426	0.61	-1.80	-5.41	-3.00
2f	348	0.55	-1.85	-5.35	-2.95
2g	400	0.75	-1.74	-5.55	-3.06
2h	373	0.60	-1.74	-5.40	-3.06

^a Decomposition temperature. ^b Anodic Peak Potential, irreversible. ^c Reduction Potential, reversible.

**Figure 1.** Perspective view of **2c**. (Thermal ellipsoids at 30% probability, hydrogen atoms and solvent molecules omitted for clarity.)

Results of thermogravimetric analysis (Table 1) showed that **2e** is the most stable. This is an interesting observation given that, for most cyclometalated Pt(II) emitters used in OLEDs, the ligated Cl complex has usually been employed as a precursor for subsequent material preparation.^{6,9} The thermal stabilities of **2a–2h** (Table 1) are comparable to that of [(C \wedge N \wedge N)Pt(C \equiv C) $_n$ R] ($n = 1–4$; R = aryl, SiMe $_3$; $T_d \approx 400$ °C),⁶ while being slightly lower than those of the [Pt(N $_2$ O $_2$)] complexes ($T_d = 440–530$ °C).²

The structure of **2c** was determined by X-ray crystal analysis (Figure 1).¹⁰ In **2c**, the Pt atom adopts a distorted square-planar geometry. The slight distortion is revealed by the \angle O1–Pt–N1 (95.7(2)°), N1–Pt–N2 (82.0(2)°), O1–Pt–Cl (87.3(2)°), and N2–Pt–Cl (95.1(2)°). The Pt–N distances are 1.979(7) and 2.006(6) Å, and the Pt–O and Pt–Cl distances are 1.972(5) and 2.311(2) Å, respectively. These values are comparable to those for [Pt(N $_2$ O $_2$)] (mean Pt–N = 1.960 and 1.978 Å, mean Pt–O = 1.963 and 1.975 Å)² and **2a**·CH $_2$ Cl $_2$ (Pt–O \approx 1.95 Å, Pt–N \approx 2.00 Å, Pt–Cl \approx 2.32 Å).¹¹

In DMF, **2a–2e**, **2g**, and **2h** exhibit an intense absorption at $\lambda_{\text{max}} \approx 300$ nm ($\epsilon > 10^4$ mol $^{-1}$ dm 3 cm $^{-1}$), moderately intense bands at 366–371 nm, and a shoulder at 381–388 nm ($\epsilon \approx (0.5–0.7) \times 10^4$ mol $^{-1}$ dm 3 cm $^{-1}$, Table 2). For

Table 2. Photophysical Data for **2a–2h**

	λ_{max} , abs ^a /nm ($\epsilon/\times 10^4$ mol $^{-1}$ dm 3 cm $^{-1}$)	λ_{max} , PL-DMF ^b / nm	λ_{max} , PL ^c /nm ($\tau/\mu\text{s}$, Φ^g), 298 K	λ_{max} , PL ^c /nm ($\tau/\mu\text{s}$), 77 K	λ_{max} , PL ^d /nm ($\tau/\mu\text{s}$), 77 K	λ_{max} , PL ^e /nm
2a	301 (1.11) 370 (0.46) 386 (0.36) 455 (0.18)	606	634 (1.2, 0.01)	556, 606 (11.6)	545, 586 (23.5)	571
2b	300 (1.98) 367 (0.68) 318 (0.63) 407 (0.45) 415 (0.28)	600	609 (1.1, 0.02)	577, 607 (20.4)	544, 582 (35.6)	564
2c	301 (1.98) 366 (0.71) 381 (0.65) 406 (0.48) 450 (0.30)	593	543, 580 (1.0, 0.03)	564, 600 (16.5)	521, 553 (24.2)	570
2d	301 (2.01) 371 (0.60) 386 (0.59) 417 (0.47) 462 (0.35)	618	598 (1.4, 0.01)	586, 633 (15.8)	540, 574 (20.9)	580
2e	302 (1.61) 366 (0.47) 382 (0.48) 424 (0.42) 465 (0.24)	606	555, 579 (1.6, 0.04)	559, 605 (16.0)	526, 557 (18.6)	574
2f	279 (2.87) 384 (0.97) 460 (0.34)	600	550, 584 (1.0, 0.01)	560, 604 (11.8)	518 (10.6)	574
2g	301 (1.20) 367 (0.46) 387 (0.41) 438 (0.27)	596	–	–	–	–
2h	301 (1.20) 366 (0.46) 388 (0.41) 412 (0.33) 439 (0.26)	595	–	–	–	–

^a Absorbance. ^b Photoluminescence in DMF solution (10 $^{-5}$ M). ^c Photoluminescence in the solid state. ^d Photoluminescence in MeOH/EtOH (4:1) glass. ^e Photoluminescence in doped film (PVK (poly(*N*-vinylcarbazole)/Pt(II) complex (5%)). ^f Lifetime. ^g Quantum yield.

2f, there are two intense absorptions at 279 nm ($\epsilon \approx 3 \times 10^4$ mol $^{-1}$ dm 3 cm $^{-1}$) and 384 nm ($\epsilon \approx 1 \times 10^4$ mol $^{-1}$ dm 3 cm $^{-1}$). With reference to previous works on [Pt(N $_2$ O $_2$)]² and [Pt(qol) $_2$] (qol = 8-quinolinolato-*O,N*),¹² the absorption at $\lambda_{\text{max}} \approx 300$ nm is attributed to a ligand-centered ($1 \rightarrow \pi^*$) ($1 =$ lone pair/phenoxide) transition, whereas the moderately intense band at 360–400 nm is attributed to $^1[1 \rightarrow \pi^*(\text{diimine})]$ mixed with Pt($d\pi$) \rightarrow $\pi^*(\text{diimine})$ charge-transfer transitions.^{2,12} The absorption spectra of **2e** in DMF and CH $_2$ Cl $_2$ are similar, but in C $_6$ H $_6$, the absorption bands are red-shifted (λ_{max} at 302, 366, 382, and 424 nm in DMF; 312, 386, 409, and 439 nm in C $_6$ H $_6$).

At room temperature, excitation ($\lambda = 385–452$ nm) of **2a–2h** in DMF solutions results in a broad orange-red emission (λ_{max} at 593–618 nm, Table 2). The quantum yields were too low to be measured; presumably, this is due to quenching by DMF. The emission energies of **2a–2h** are red-shifted compared to those of the related [Pt(N $_2$ O $_2$)]

(9) Lu, W.; Chan, M. C. W.; Zhu, N.; Che, C. M.; Li, C.; Hui, Z. *J. Am. Chem. Soc.* **2004**, *126*, 7639–7651.

(10) CCDC 261410 contains the supplementary crystallographic data for **2c** in this paper. These data can be obtained free of charge via www.ccdc.cam.ac.uk/data_request/cif; by e-mailing data_request@ccdc.cam.ac.uk; or by contacting The Cambridge Crystallographic Data Centre, 12, Union Road, Cambridge CB2 1EZ, UK (fax: +44 1223 336033).

(11) Bardwell, D. A.; Crossley, J. G.; Jeffery, J. C.; Orpen, A. G.; Psillakis, E.; Tilley, E. E. M.; Ward, M. D. *Polyhedron* **1994**, *13*, 2291–2300.

(12) Donges, D.; Nagle, J. K.; Yersin, H. *Inorg. Chem.* **1997**, *36*, 3040–3048.

Table 3. EL Data for **2a–2e**

device	λ_{\max} / nm	CIE ^a x, y	x/% ^b	B_{\max} /cd m ⁻² (V/V) ^c	Eff _{max} /cd A ⁻¹ (J/mA cm ⁻²) ^d
A (2a)	564	0.48, 0.50	6	6000 (16)	2.9 (4.4)
B (2b)	565	0.51, 0.48	5	14000 (16)	9.7 (4.2)
C (2c)	564	0.50, 0.49	6	26000 (14)	13 (1.4)
D (2d)	572	0.53, 0.46	6	10000 (19)	7.3 (2.9)
E (2e)	566	0.48, 0.51	5	37000 (16)	7.8 (89)

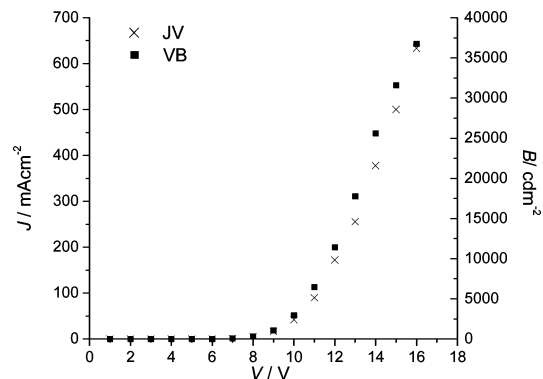
^a 1931 Commission Internationale de l'Éclairage coordinates. ^b Dopant percentage of **2a–2e**. ^c Maximum brightness (B_{\max}) achieved at the voltage V. ^d Maximum current efficiency (Eff_{max}) achieved at the current density J.

complexes (589 nm)² but blue-shifted from that of [Pt(qol)₂] (650 nm).¹² With reference to previous works on [Pt(N₂O₂)]² and [Pt(qol)₂],¹² the emission of [(O \wedge N \wedge N)PtX] is tentatively attributed to come from triplet excited state with mixed ³MLCT and ³[l \rightarrow π^* (diimine)] (l = lone pair/phenoxide) parentage. Solvent effect on the emission was examined using **2e** as an example. Its emission λ_{\max} is relatively solvent insensitive, but the emission lifetime (τ) is affected by the solvent (0.27 μ s in CH₂Cl₂ and 0.41 μ s in C₆H₆; the emission lifetime in DMF was too short to be measured). In CH₂Cl₂, the self-quenching rate constant for the emission of **2e** is 3.6×10^8 mol⁻¹ dm⁻³ s⁻¹.

Cyclic voltammograms of **2a–2h** in DMF show an irreversible oxidation wave with E_{pa} at 0.60–0.86 V and a reversible reduction couple with $E_{1/2}^{\text{red}}$ between -1.69 and -1.85 V versus [Cp₂Fe]⁺⁰. The HOMO and LUMO levels of these complexes were estimated to be in the ranges from -5.35 to -5.66 eV and from -2.95 to -3.11 eV, respectively (Table 1).

OLEDs with the following configuration were prepared for **2a–2e**: ITO (indium tin oxide)/NPB (4,4'-bis[N-(1-naphthyl)-N-phenylamino]biphenyl, 40 nm)/CBP (4,4'-N,N'-dicarbazolebiphenyl):Pt(II) complex (x%, 30 nm)/BCP (2,9-dimethyl-4,7-diphenyl-1,10-phenanthroline, 20 nm)/Alq₃ (tris(8-quinolinolato)aluminum, 30 nm)/LiF (0.5 nm)/Al (100 nm). A data summary for the devices achieved using optimized **2a–2e** doping concentrations is provided in Table 3.

Devices A–E are yellow-light-emitting with similar CIE coordinates (Table 3). The electroluminescence (EL) λ_{\max} for all complexes is independent of their doping concentrations, and the band shape is similar to that of photoluminescence (PL), although the EL emission is blue-shifted, presumably because of solvent relaxation and doping (Tables 2 and 3). The device performance (E > C > B > D \approx A, Table 3) follows a trend similar to those of the emission quantum yield (Φ of **2e** > **2c** > **2b** > **2d** \approx **2a**, Table 2) and thermal stability (T_d of **2e** \approx **2c** \approx **2b** > **2d** \approx **2a**, Table 1) of the complex. In particular, the complexes with bulky groups and F substituent on the (O \wedge N \wedge N) ligand gave better devices. There is, however, no correlation between device performance and the emission lifetime of the complexes. Complex **2e** gave the device (E) with the best performance; this device gave a brightness of 1 cd m⁻² at 4 V, and the maximum current efficiency of 7.8 cd A⁻¹ was obtained at

**Figure 2.** J - V - B (current density–voltage–brightness) relationships for device E.

89 mA cm⁻². The device was stable in terms of efficiency decay, and the efficiency was attained at 5.8 cd A⁻¹ when the current density was increased to 633 mA cm⁻². The maximum brightness of 37000 cd m⁻² was achieved at 16 V (Figure 2), which is higher than those of the yellow OLEDs with [(C \wedge N \wedge N)PtR]⁺ (maximum luminance = 7800 cd m⁻², λ_{\max} = 564 nm),⁶ [Pt(N₂O₂)] (4480 cd m⁻², CIE x = 0.42, y = 0.56),² Pt Schiff base emitters (23000 cd m⁻², CIE x = 0.48, y = 0.52),³ and other non-Pt emitters in the literature.^{13–15}

In summary, we have demonstrated [(O \wedge N \wedge N)PtX] complexes to be robust phosphorescent materials for OLEDs with good performance. Their preparation and structural modification are simple.^{6,9,16,17} The physical properties of these complexes, such as T_d and band gap, can also be easily modified through the non-chelated site on the Pt atom.

Acknowledgment. We gratefully acknowledge the financial support by the University Development Fund (Nanotechnology Research Institute, 00600009) of The University of Hong Kong and Innovation and Technology Commission of The Government of Hong Kong Special Administrative Region (HKSAR), China (Project No. ITS/53/01). We would also like to thank Sunic System Ltd. for support on fabrication techniques.

Supporting Information Available: Experimental procedures, thermogravimetric analysis, X-ray crystal data of **2c**, UV–vis and PL spectra of **2a–2h** in DMF, spectra depicting solvent effect on the absorption of **2e**, cyclic voltammograms of **2a–2h**, and EL spectra and J - V - B plots of devices A–D. This material is available free of charge via the Internet at <http://pubs.acs.org>.

IC050365Q

- Lin, X. Q.; Chen, B. J.; Zhang, X. H.; Lee, C. S.; Kwong, H. L.; Lee, S. T. *Chem. Mater.* **2001**, *13*, 456–458.
- Lamansky, S.; Djurovich, P.; Murphy, D.; Abdel-Razzaq, F.; Lee, H.-E.; Adachi, C.; Burrows, P. E.; Forrest, S. R.; Thompson, M. E. *J. Am. Chem. Soc.* **2001**, *123*, 4304–4312.
- Mazzeo, M.; Pisignano, D.; Favaretto, L.; Barbarella, G.; Cingolani, R.; Gigli, G. *Synth. Met.* **2003**, 671–673.
- Lai, S. W.; Chan, M. C. W.; Cheung, K. K.; Che, C. M. *Organometallics* **1999**, *18*, 3327–3336.
- Wong, K. H.; Chan, M. C. W.; Che, C. M. *Chem. Eur. J.* **1999**, *5*, 2845–2849.